

The Absorption Spectrum of Rhodonite

MARC MARSHALL, AND W. ALAN RUNCIMAN

*Department of Solid State Physics, Research School of Physical Sciences,
Australian National University,
Canberra, A.C.T. 2600, Australia*

Abstract

The absorption spectra of pieces of a high-iron, high-calcium rhodonite crystal have been measured for incident polarized radiation with the electric vector parallel to the principal axes of the refractive index indicatrix, in the range 4500 to 31000 cm^{-1} at 18 K and from 2000 to 30000 cm^{-1} at room temperature. Absorption spectra of crystals of the same rhodonite and of a low-iron, low-calcium rhodonite were taken over the same ranges, with the electric vector of the incident light parallel to the axes of the indicatrix section parallel to (100). The change in the axis directions with wavelength between 16000 and 31000 cm^{-1} for the (100) slice of low-iron rhodonite is described; the change for the high-iron rhodonite principal axes between 2000 and 31000 cm^{-1} was within the limits of error. Powder spectra of the two rhodonites and of a low-iron, high-calcium rhodonite were taken between 300 and 2000 cm^{-1} . Band wavenumbers at 18 K and room temperature plus the intensities and polarization ratios for the high-iron rhodonite at 18 K have been tabulated. Comparisons among the powder spectra permit the vibrational bands to be assigned to various groups of sites. Comparing the high- and low-iron rhodonite crystal spectra permits most non-vibrational bands to be assigned to Fe^{2+} or Mn^{2+} $d \rightarrow d$ transitions. The approximate symmetry of the preferred Fe^{2+} site $M(4)$ was used as a basis for classification of the Fe^{2+} bands.

Introduction

Previous authors have measured, at room temperature, the powder absorption spectrum of low-iron rhodonite between 250 and 2000 cm^{-1} (*e.g.*, Lazarev and Tenisheva, 1961; Agiorgitis, 1969; Rutstein and White, 1971) and the unpolarized absorption spectra between 4000 and 30000 cm^{-1} of 10 weight percent Fe rhodonite crystals (Keester and White, 1968) and 3 percent Fe rhodonite crystals (Manning, 1968). The unpolarized absorption spectrum between 10500 and 50000 cm^{-1} of a rhodonite crystal of unstated iron content was measured at room temperature and 90 K by Lakshman and Reddy (1972).

This paper extends these measurements in two ways. The powder absorption spectra of high-iron rhodonite and low-iron rhodonites of different calcium contents between 300 and 2000 cm^{-1} were measured at room temperature to ascertain the effects of iron and calcium. The three polarized absorption spectra for the principal axes of the refractive index indicatrix of a high-iron rhodonite crystal and the polarized absorption spectra for light normally incident on the (100) plane of low-

iron and of high-iron rhodonite crystals were measured between 4500 and 31000 cm^{-1} at 18 K and between 2000 and 30000 cm^{-1} at room temperature. Using rhodonites of different iron contents permits an unambiguous distinction to be made between iron and manganese bands while polarized and low temperature spectra reveal weak bands not observed before and provide evidence for deciding band assignments.

Material

Rhodonite, $(\text{Mn,Ca,Fe})\text{SiO}_3$, is a triclinic pyroxenoid silicate with space group $P\bar{1}$. From the work of Peacor and Niizeki (1963) it is presumed that Ca prefers the $M(5)$ site, while the other metallic cations are distributed among the $M(1)$, $M(2)$, $M(3)$, and $M(4)$ sites which are in distorted octahedral coordination with oxygen sites and have site symmetry C_1 . In low-calcium rhodonite, Mn^{2+} will occupy $M(5)$ also.

The high-iron rhodonite sample, a single crystal, came from Level 17, 128 ft. contour, Zinc Corporation Mine, Broken Hill, New South Wales. Its pycnometric density was 3.62 g cm^{-3} . Overton

(1968) measured the crystallographic and optical properties of a crystal of similar source and composition, expressing his results in terms of the unit cell defined by Gossner and Brückl (1928). He found $a = 7.67 \text{ \AA}$, $b = 12.21 \text{ \AA}$, $c = 6.68 \text{ \AA}$, $\alpha = 85.3^\circ$, $\beta = 93.9^\circ$ and $\gamma = 111.7^\circ$. This is the unit cell used below unless otherwise stated.

The principal axes of the refractive index indicatrix may be specified by the longitude ϕ and co-latitude ρ of the direct projections of the axes on a sphere. (See Bloss, 1971, Chapter IV, for a discussion of the conventions used in making such projections.) Overton found that the average ϕ and ρ values in the visible of the principal axes of the refractive index indicatrix were:

$$X; \phi = 275.6^\circ, \rho = 43.8^\circ$$

$$Y; \phi = 24.2^\circ, \rho = 73.2^\circ$$

$$Z; \phi = 127.9^\circ, \rho = 51.0^\circ.$$

The low-iron, low-calcium rhodonite was obtained from World-Wide Gem Rough, Sydney, New South Wales, as a lump of massive material with crystals about 1 mm in dimension embedded in it. It came from Danglemar in the district of Tamworth, New South Wales. The low-iron, high-calcium rhodonite, which showed no distinguishable crystals, came from Cornwall, U.K.

The rhodonites were analyzed for elements between Na and Zn inclusive in the periodic table by electron microprobe analysis, the proportions being expressed as weight percent of the oxides (Table 1). Chemical analyses of Broken Hill rhodonite (Deer, Howie, and Zussman, 1963, p. 185) gave an $\text{Fe}^{3+}/\text{Fe}^{2+}$ ratio of less than 0.01.

Method

300 to 2000 cm^{-1}

KBr discs of diameter 13 mm containing 2.7 mg of high-iron or low-iron, high-calcium rhodonite or

TABLE 1. Electron Microprobe Analyses of Rhodonite

SiO ₂	MnO	CaO	FeO	MgO	TiO ₂	Other	Total
High-iron (Broken Hill)							
46.71	31.64	9.04	12.46	0.32	- -	<0.1 each	100.17
Low-iron (Danglemar)							
46.35	50.60	1.85	<0.15	0.38	0.12	<0.1 each	99.30
Low-iron (Cornwall)							
46.03	44.75	7.14	2.14	0.49	- -	<0.1 each	100.55

3.1 mg of low-iron, low-calcium rhodonite were pressed and their spectra scanned at room temperature with a Perkin-Elmer Model 180 spectrophotometer. Each spectrum was compared with that of a pure KBr disc, and bands common to both removed from the rhodonite spectra.

2000 to 31000 cm^{-1}

For simplicity, the experimental conditions should be such that the absorbance for any polarization and transition is proportional to the square of the cosine of the angle between the electric vector of the light and the transition moment. Starting with the relation between transition moments and the conductivity tensor quoted by Ward (1955) and using the formulae for light propagation in absorbing anisotropic media given by Ramchandran and Ramaseshan (1961), one may show that suitable experimental conditions are:

(1) the incident beam is parallel to a principal axis of the refractive index indicatrix and is linearly polarized with the electric vector parallel to another principal axis,

$$(2) \quad |(1/n_1^2) - (1/n_2^2)| \gg k\lambda/2\pi n^3,$$

where n_1, n_2 are the refractive indices for the principal axes of the refractive index indicatrix at right angles to the propagation direction, k is the absorption coefficient, λ is the vacuum wavelength, and n is the refractive index of the wave travelling through the crystal.

In rhodonite, provided that condition (1) be satisfied, $k\lambda/2\pi n^3$ between 16000 and 31000 cm^{-1} is less than 0.1 percent of $|(1/n_1^2) - (1/n_2^2)|$. The difference between n_1 and n_2 will probably fall with decreasing wave-number, but should remain sufficiently large for condition (2) to be satisfied down to 2000 cm^{-1} .

For condition (1) to be satisfied, the directions of the principal axes of the refractive index indicatrix must first be found. As rhodonite is triclinic, an experimental approach is necessary; this was only feasible for the high-iron rhodonite.

Two pieces of the high-iron rhodonite crystal were cut, one with a pair of parallel faces normal to one of the principal axes of the refractive index indicatrix measured by Overton (1968), the other with two pairs of parallel faces normal to the other two axes. The absorption spectra between 2000 and 30000 cm^{-1} at room temperature and between 4500 and 31000 cm^{-1} at $18 \pm 3 \text{ K}$ were measured with

each of the three pairs of parallel faces normal to the beam, spectra being taken for each pair with various polarizer settings in a 180° range. A Cary Model 17 spectrophotometer was used between 4200 and 31000 cm^{-1} and, for the 18 K runs, the crystal was in a flow tube with a fused silica section. The Perkin-Elmer Model 180 spectrophotometer was used between 2000 and 4200 cm^{-1} .

At each temperature and wavelength, the axis directions for the refractive index indicatrix section at right angles to the incident wave-normal were found from the condition that these axes are parallel to the directions of the incident light electric vector which give maximum and minimum absorption (Ward, 1955). Within the limits of experimental error, the axis directions so found agreed with those expected from Overton's measurements (1968) at all wavelengths and temperatures, so that the directions of the indicatrix principal axes could be deduced. The experimental errors are such that the directions taken as the principal axis directions may differ by up to 20° from the true principal axis directions. The required spectra were chosen from those taken; the spectra parallel to X , Y , and Z in the visible are labelled α , β , and γ respectively.

Danglemar low-iron rhodonite crystals were too small for principal axis pieces to be cut. A (100) cleavage slice was used; the axes of the indicatrix section parallel to (100) were found as before and spectra taken in the same ranges. For comparison, spectra were taken for a high-iron rhodonite (100) cleavage slice.

Results

The (100) cleavage slice of high-iron rhodonite was larger than the principal axis pieces so that stricter limits could be placed on the variation of axis direction with wavelength. Between 2000 and 30000 cm^{-1} the variation was less than 10° , and the axis directions agreed within 5° with those deduced from the measurements of Overton (1968). For the Danglemar low-iron rhodonite (100) cleavage slice, the acute angle between one of the axis directions and the b axis in the range 21000-30000 cm^{-1} was $10 \pm 3^\circ$ lower than the value of $20 \pm 5^\circ$ found between 16000 and 20000 cm^{-1} ; the corresponding high-iron rhodonite angle was 40° . (The small absorption of low-iron rhodonite below 16000 cm^{-1} results in a large error in axis direction, so no changes could be detected below 16000 cm^{-1} .)

Figure 1 shows the high-iron rhodonite powder spectrum and Figures 2-4 the high-iron crystal spectra. The 8000-30000 cm^{-1} room temperature spectra, which gave little additional information, are not shown. The powder spectra for the low-iron rhodonites resembled those previously published. Figure 5 shows the polarized spectra of the high-iron rhodonite and the Danglemar low-iron rhodonite for normal incidence on the (100) cleavage plane at 18 K between 16000 and 31000 cm^{-1} . Between 2000 and 16000 cm^{-1} , the Danglemar low-iron rhodonite crystal showed only faint, ill-defined bands.

The rhodonite powder spectra differ from each other below 490 cm^{-1} in the positions of corresponding bands. The crystal spectra reveal a few unreported bands and give the polarization properties of the bands. Cooling the crystal increases the number of observable bands and defines band polarizations more clearly.

Band positions listed in Table 2 were obtained from the observed peak positions where possible. The accuracy of the observed peak positions is indicated by the number of significant figures given. When two wavenumbers are given for a band they are the maximum and minimum wavenumbers of the observed peak in different polarizations.

Certain bands listed do not give observed peaks

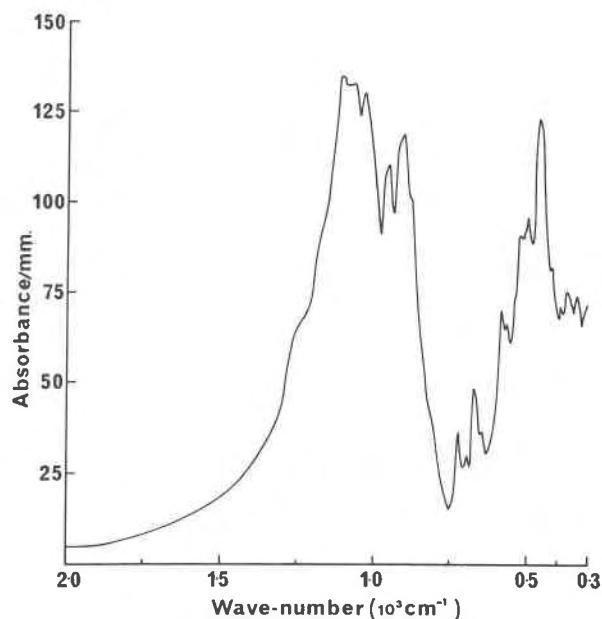


FIG. 1. Room temperature unpolarized spectrum of high-iron, high-calcium rhodonite from 300-2000 cm^{-1} .

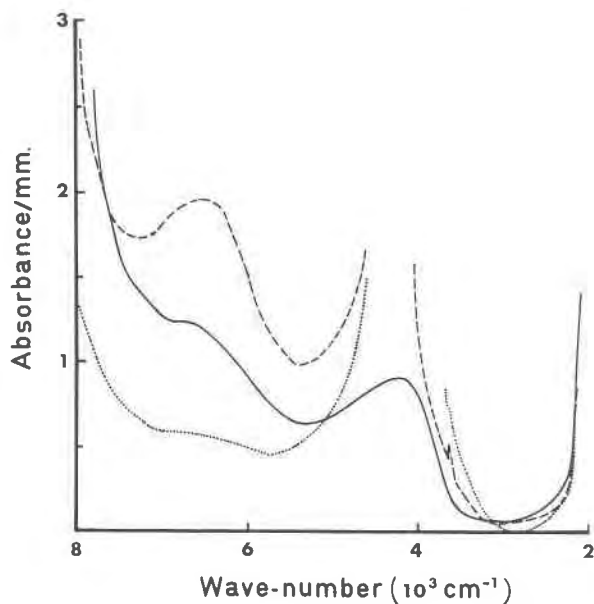


FIG. 2. Room temperature spectra of rhodonite from 2000 to 8000 cm^{-1} . \cdots α spectrum, $---$ β spectrum, $—$ γ spectrum.

or shoulders. The α and β intensities are almost the same on the low-energy side of the 9700 cm^{-1} band, but diverge at higher energies, suggesting that the "band" is the envelope of two bands near 8000 and 9800 cm^{-1} respectively at 18 K. The high-iron

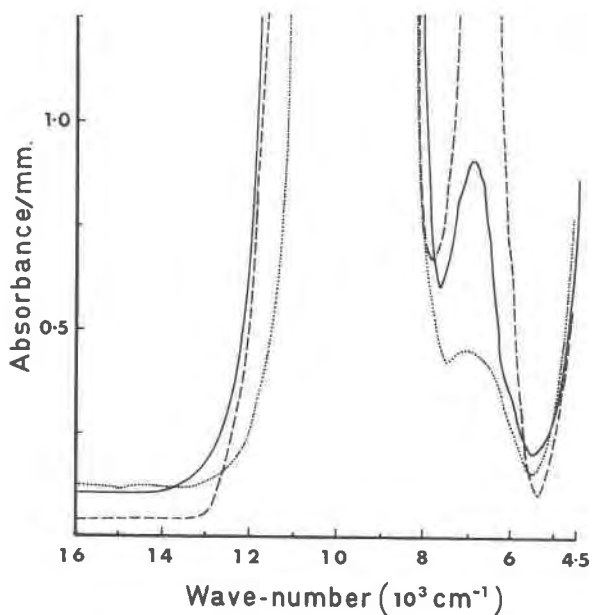


FIG. 3. 18 K spectra of rhodonite from 4500 to 16000 cm^{-1} . \cdots α spectrum, $---$ β spectrum, $—$ γ spectrum.

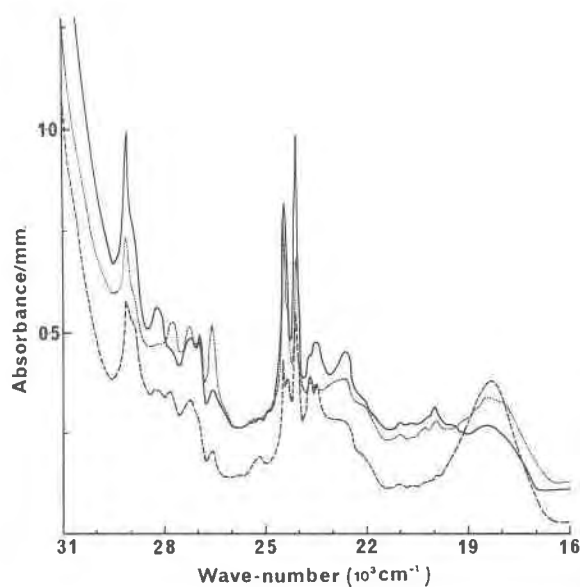


FIG. 4. 18 K spectra of rhodonite from 16000 to 31000 cm^{-1} . \cdots α spectrum, $---$ β spectrum, $—$ γ spectrum.

rhodonite band at 23000 cm^{-1} is required to explain differences between the shapes of the α and γ high-iron rhodonite spectra.

The intensities and polarization ratios for the high-iron rhodonite have an absolute significance and are also given in Table 2. Where possible they were calculated from the 18 K data, as the bands are better resolved. Experiments showed that the maximum intensity error from errors in the indicatrix principal axes was 25 percent and for most bands was much less; the errors in polarization ratios are smaller. A more important cause of uncertainty is uncertainty in band size and shape; the extreme right-hand column of Table 2 gives estimates of the uncertainties from this cause in the polarization ratios. The fractional uncertainties in the total intensities will follow the same trends as the uncertainties in the polarization ratios, but will be larger. The intensities of the bands at 8000 and 9800 cm^{-1} cannot be separated, so the sum of their intensities is given in Table 2.

Band Assignments

300 to 4000 cm^{-1}

Band positions between 490 and 1100 cm^{-1} are the same within 3 cm^{-1} for the three rhodonites studied, but the positions of corresponding bands

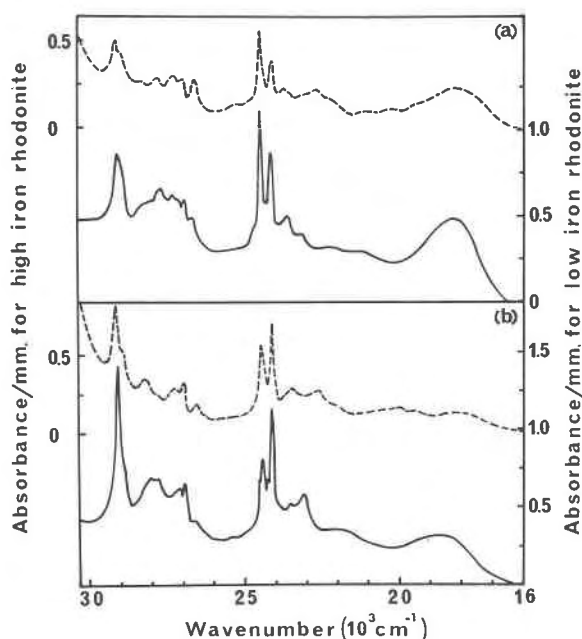


FIG. 5. Comparison between 18 K polarized spectra of high-iron, high-calcium rhodonite (dashed line) and low-calcium, low-iron rhodonite (solid line) for light incident normal to (100). (a) Acute angle between electric vector of incident light and b axis = $80\text{--}50^\circ$. (b) Acute angle between electric vector of incident light and b axis = $10\text{--}40^\circ$.

between 330 and 470 cm^{-1} for the high-iron rhodonite differ by $10\text{--}20\text{ cm}^{-1}$ from those for the low-iron rhodonites. Since the rhodonites differ mainly in the types of ions occupying $M(1)\text{--}M(5)$, this result suggests that bands between 490 and 1100 cm^{-1} come from vibrations heavily involving silicate groups, while those between 330 and 470 cm^{-1} come from vibrations heavily involving ions at some or all of $M(1)\text{--}M(5)$; a similar assignment was made by Lazarev and Tenisheva (1961). The positions of some bands between 330 and 470 cm^{-1} are the same for low-iron, low-calcium and low-iron, high-calcium rhodonite; such bands probably come from vibrations heavily involving ions at some or all of $M(1)\text{--}M(4)$, the preferred iron sites, and not involving $M(5)$.

The 1180 and 1260 cm^{-1} bands are probably combination bands of the strong SiO_4 and low frequency modes. The position and width of the 3625 cm^{-1} band are characteristic of an OH stretching vibration and the polarization of the band suggests the OH groups are at definite sites relative to the lattice, a suggestion supported by Wilkins and Sabine (1973).

4000 to 31000 cm^{-1}

Charge-Transfer Bands. Fe-O and Mn-O charge-transfer bands have not been observed in this region, but metal-metal bands could be important (Allen and Hush, 1967); the microprobe analyses show that the most intense will probably involve pairs chosen from Mn and Fe in different charge states.

Comparison of the experimental high-iron rhodonite band polarizations with those theoretically predicted for charge-transfer bands will indicate which observed bands could be due to charge transfer. The band intensities in the α , β , and γ spectra will be proportional to the squares of the cosines of the angles between the transition moment of the band and the X , Y , and Z directions respectively. (This neglects the ratio of refractive indices, but for rhodonite the error is less than 1 percent.) Under certain assumptions Hush (1967, p. 437) showed that the transition moment for an allowed charge-transfer transition will be directed along the line joining the two ions. Therefore, in this situation the theoretical polarization ratios can be calculated if the atomic coordinates for the crystal structure, the direction cosines of X , Y , and Z , and the sites occupied by the charge-transfer ions are known.

The trivalent ions are smaller than the divalent ions but much larger than Si^{4+} so that they will probably prefer $M(4)$ to the other cation sites. The divalent ions participating in charge transfer could be at any of $M(1)\text{--}M(4)$. Thus, the charge-transfer band transition moment will probably lie along the line joining $M(4)$ to a neighboring $M(1)$, $M(2)$, $M(3)$, or $M(4)$ site. Atomic coordinates for high-iron rhodonite have not been measured, so that one must make the approximation of using the coordinates for low-iron rhodonite. Table 3 gives predicted ratios using the atomic coordinates of Peacor and Niizeki (1963) and the X , Y , and Z determined by Overton (1968), together with the bands which have the required polarization ratios.

The 6900 cm^{-1} band is probably an $\text{Fe}^{2+} d \rightarrow d$ band (see below). The 18770 , 19130 , and 25400 cm^{-1} bands have half-widths of only $100\text{--}200\text{ cm}^{-1}$ and seem to belong to groups of bands of which other members are unlikely to be charge-transfer bands. There are no arguments against assigning the bands at $20210\text{--}20250$ and 25200 cm^{-1} to charge-transfer transitions, though the bands can be assigned without difficulty to $d \rightarrow d$ transitions. The 25200 cm^{-1} band is probably due to $M(4)\text{--}M(3)$

TABLE 2. The Rhodonite Spectrum

Low-iron rhodonite 18K	Band wavenumber (cm ⁻¹)		Assignment†	High-iron rhodonite		Error in numbers in ratio
	High-iron rhodonite 18K	Room temp.		Intensity** [(abs/cm)cm ⁻¹]	α:β:γ ratio	
		333,411, 450	Vibrations involving M(1)-M(4)			
		366,386	Vibrations involving M(1)-M(5)			
		490-1100	Vibrations involving silicate groups			
		1180, 1260	Combination vibrations			
		3625	OH stretch vibration	10	0.32:0.52:0.16	<0.03
		4250	M(4)Fe ²⁺ ; 5A' → 5A''	3.7 x 10 ⁴	0.60:0.25:0.15	<0.03
	6770-7040	6700	M(4)Fe ²⁺ ; 5A' → 5A'	3.1 x 10 ⁴	0.1 :0.7 :0.2	0.03-0.1
	8000	8000*	M(4)Fe ²⁺ ; 5A' → 5A''	1.2 x 10 ⁶	Strongest in α	0.03-0.1
	9800	9750	M(4)Fe ²⁺ ; 5A' → 5A'			
18200-18700	18310-18480	18500	Mn ²⁺ ; 6A _{1g} → 4T _{1g}	1.3 x 10 ⁴	0.34:0.44:0.22	0.01
	18770	19500*	Fe ²⁺	10	1 :0 :0	>0.1
	19130			100	1 :0 :0	>0.1
	19500-19530			7 x 10 ²	0.07:0.25:0.68	0.03-0.1
	19950-19970	20000	M(4)Fe ²⁺ ; 5A' → 3A'	1.4 x 10 ³	0.20:0.16:0.64	<0.03
	20320	20300*	Fe ²⁺	8 x 10 ²	0.45:0.22:0.33	0.03-0.1
	20680-20700	20700*		7 x 10 ²	0.20:0.28:0.52	0.03-0.1
	21000-21030			1.1 x 10 ³	0.36:0.19:0.45	0.03-0.1
	20210-20250			Fe ²⁺ or M(4)-M(4) charge transfer involving Fe ²⁺	30	0 :0 :1
21200-21500			M(5)Mn ²⁺ ; 6A _{1g} → 4T _{2g}			
21500-22200	22000-22300	22400*	Mn ²⁺ ; 6A _{1g} → 4T _{2g}	4.3 x 10 ³	0.33:0.24:0.43	<0.03
	22620-22740		M(4)Fe ²⁺ ; 5A' → 3A'	2.3 x 10 ³	0.25:0.33:0.42	0.03-0.1
23060-23120	23000	23600	Mn ²⁺ ; 6A _{1g} → 4T _{2g}	1.0 x 10 ³	0.4 :0.3 :0.5	>0.1
	23470-23510		M(4)Fe ²⁺ ; 5A' → 3A'	2.4 x 10 ³	0.24:0.32:0.44	0.03-0.1
23520-23590	23640-23660	24080	Mn ²⁺ ; 6A _{1g} → 4T _{2g}	2.6 x 10 ³	0.2 :0.5 :0.3	>0.1
24020	24020		3.7 x 10 ²	0.4 :0.4 :0.2	>0.1	
24110-24120	24070-24100		2.0 x 10 ³	0.26:0.25:0.49	<0.03	
24270-24280	24330-24360	24480	Mn ²⁺ ; 6A _{1g} → 4E _g 4A _{1g}	1.4 x 10 ³	0.33:0.28:0.39	0.03-0.1
24400-24450	24450-24470		2.3 x 10 ³	0.37:0.22:0.41	0.03-0.1	
24510			M(5)Mn ²⁺ ; 6A _{1g} → 4E _g 4A _{1g}			
24700-24800	24620-24750	25200*	Mn ²⁺	6.5 x 10 ²	0.23:0.34:0.43	0.03-0.1
24990	24950-24990			2 x 10 ²	0.4 :0.2 :0.3	>0.1
	25400			1 x 10 ²	0.6 :0 :0.4	>0.1
	25770			80	0.2 :0.7 :0.1	>0.1
25000-25400	25180-25300		M(4)-M(3) charge transfer or Mn ²⁺	4.4 x 10 ²	0.14:0.62:0.24	0.03-0.1
26610-26640	26200-26300	26600	Fe ²⁺ not at M(4)	2.5 x 10 ²	0.54:0 :0.46	0.03-0.1
	26530-26580		Mn ²⁺ ; 6A _{1g} → 4T _{2g}	1.1 x 10 ³	0.67:0.14:0.19	<0.03
26900-26940	26960-27000	27000	Mn ²⁺ ; 6A _{1g} → 4T _{2g} or Fe ³⁺	5.6 x 10 ²	0.45:0.17:0.38	<0.03
27060-27100	27210-27250		Mn ²⁺ ; 6A _{1g} → 4T _{2g}	2.7 x 10 ³	0.37:0.31:0.32	<0.03
27260			Mn ²⁺ ; 6A _{1g} → 4T _{2g}	1.8 x 10 ³	0.41:0.38:0.21	<0.03
27630-27800	27700-27840	27800	M(5)Mn ²⁺ ; 6A _{1g} → 4T _{2g}			
27950-28020			Mn ²⁺ ; 6A _{1g} → 4T _{2g}	2.1 x 10 ³	0.31:0.33:0.36:	<0.03
28200	28190-28270	29200	Mn ²⁺ ; 6A _{1g} → 4E _g	1.8 x 10 ³	0.25:0.46:0.29	0.03-0.1
28840-28920	28850-28890		3.5 x 10 ³	0.26:0.24:0.50	<0.03	
29030-29050	29100-29130					

* Room temperature band not previously reported.

† For Mn²⁺ electronic transitions the corresponding octahedral transition is given.** To convert to oscillator strengths, multiply by 2.7 x 10⁻¹⁰ for Mn²⁺ bands, 6.9 x 10⁻¹⁰ for Fe²⁺ bands. The oscillator strengths so obtained are calculated for the total concentration of the appropriate ion in rhodonite.

TABLE 3. Charge-Transfer Bands

Sites of participating ions	Expected $\alpha:\beta:\gamma$ ratio	Wavenumber of bands with correct $\alpha:\beta:\gamma$ ratio (cm^{-1})
M(4), M(3)	0.04:0.67:0.29	25200
M(4), M(1)	0.78:0.03:0.19	18770, 19130, 25400
M(4), N(1)	0.55:0.40:0.05	
M(4), M(4)	0:0.13:0.87	20210-20250
M(4), M(2)	0.12:0.63:0.25	6900, 25200

rather than $M(4)$ - $M(2)$ charge transfer, as the former are much closer (3.37 Å compared to 5.85 Å) and are bridged by oxygen ions.

Iron Bands. Bands present in high-iron, but not in low-iron rhodonite, are probably due to iron. As there is little Fe^{3+} present and rhodonite analyses show no systematic trend in Fe^{3+} content with total iron content (Deer, Howie, and Zussman, 1963, p. 185-186), it is probable that most such bands are due to $\text{Fe}^{2+} d \rightarrow d$ transitions or charge-transfer transitions involving Fe^{2+} , as indicated in Table 2. In making comparisons between the polarized spectra of the two rhodonites, one must note that because of the differences between the refractive index indicatrices, polarization ratios will only be similar, not the same.

Band assignments are straightforward, except in the following cases. The ratio of intensities in different polarizations shows that the 23520-23590 cm^{-1} band in Danglemar low-iron rhodonite corresponds to the 23640-23660 cm^{-1} band in high-iron rhodonite so that the 23470-23510 cm^{-1} band is due to Fe^{2+} ; in this case band positions are not decisive. Position implies that the 23060-23120 cm^{-1} band in Danglemar low-iron rhodonite corresponds to the band at 23000 cm^{-1} in high-iron rhodonite, while polarization ratios suggest that it corresponds to the 22620-22740 cm^{-1} band in high-iron rhodonite; no other corresponding bands are as much as 400 cm^{-1} apart and the polarization ratios are uncertain, so that it is probably the 22620-22740 cm^{-1} band which is due to Fe^{2+} .

$M(4)$ is preferred by Fe^{2+} over $M(1)$ - $M(3)$ and is the most distorted of the $M(1)$ - $M(4)$ sites (Peacor and Niizeki, 1963) so that the intensity and polarization ratio of the stronger $\text{Fe}^{2+} d \rightarrow d$ bands will be dominated by $M(4)$ Fe^{2+} . However, other sites will contribute, broadening the bands and changing polarization ratios.

The $M(4)$ $d \rightarrow d$ Fe^{2+} spectrum should consist of the four bands produced by the spin-allowed

transitions from the lowest quintet state to the four remaining quintet states augmented by many weak higher-energy bands from spin-forbidden transitions. The intensities of the 4200, 8000, and 9800 cm^{-1} bands compared to those of the other Fe^{2+} bands suggest that the former are due to the spin-allowed transitions, the latter to spin-forbidden transitions. The 6900 cm^{-1} band position, intensity and, as will be seen below, polarization, are consistent with its being due to the fourth spin-allowed transition. The band polarization is also consistent with that for a charge-transfer band; but this assignment is less likely because the absence of a fourth spin-allowed transition would have to be explained and because the sites of the ions participating in the charge transfer would be 5.85 Å apart and would not be connected directly by oxygen bridges.

A finer classification of the $M(4)$ Fe^{2+} bands may be made by comparing the experimental band polarization ratios with those predicted using the approximate symmetry of the crystal field at $M(4)$. It suffices to consider the approximate symmetries of the octahedron of oxygen neighbors of $M(4)$.

As for the charge-transfer calculations, one must use the low-iron rhodonite atomic coordinates given by Peacor and Niizeki (1963). The symmetry element of the oxygen octahedron least perturbed by its distortion from a regular octahedron is the reflection plane which would include the axis O(5)-O(8) and bisect O(6)-O(9) and O(7)-O(11) if the oxygens formed a regular octahedron. The position of the plane was found by choosing the plane so that the sum of the squares of the distances that the oxygens had to move in order to make the plane an exact plane of symmetry was a minimum.

The approximate symmetry group is then C_s with irreducible representations A' and A'' . The moment for a transition between an A' and an A'' state will be perpendicular to the reflection plane, while the moment for a transition between two A' or two A'' states will lie in the plane. The expected polarization ratios for the high-iron rhodonite spectra may then be calculated as for the charge-transfer bands.

For transitions between A' and A'' states, the calculated $\alpha:\beta:\gamma$ intensity ratio is 0.60:0.22:0.18. The direction cosines (ℓ, m, n) relative to X, Y, Z for other transition moments must satisfy $0.78\ell - 0.46m + 0.42n = 0$; this relation prevents such bands from being strongly α -polarized. The strong Fe^{2+} band at 4200 cm^{-1} , which is α -polarized, has

an $\alpha:\beta:\gamma$ ratio of 0.60:0.25:0.15. To test whether the ratios for bands not α -polarized were consistent with the relation they had to satisfy, the square roots of the ratios in Table 2 were calculated, giving ($|\ell|$, $|m|$, $|n|$); $0.78|\ell| \pm 0.46|m|$ was calculated and compared with $0.42|n|$. If one of $0.78|\ell| \pm 0.46|m|$ was equal to $0.42|n|$ within experimental error, it was concluded that the relation was satisfied.

The relation was very well satisfied by the bands at 6900 cm^{-1} and $19950\text{--}19970\text{ cm}^{-1}$, and moderately well satisfied by the bands at 9800 , $22620\text{--}22740$, and $23470\text{--}23510\text{ cm}^{-1}$. For the band at 8000 cm^{-1} the polarization is not well enough determined for comparisons to be meaningful. In view of the approximations and errors, the agreement between theory and experiment appears sufficiently close to justify labelling the bands as arising from transitions between C_s states. The calculated intensity ratios for higher approximate symmetries disagree completely with experiment.

The C_s label for the ground state may be found by considering which C_s states correspond to a given O_h state. Such a correlation is given by descent-of-symmetry tables as in Wilson, Decius, and Cross (1955). If the oxygen octahedron be deformed to D_{4h} symmetry, the C_4 axis will be O(5)–O(8) and the C_2 axes which in a regular octahedron would be C_4 axes will be O(9)–O(11) and O(6)–O(7). Accordingly, the reflection plane is a σ_d plane for D_{4h} symmetry; from tables it then follows that the O_h quintet Fe^{2+} states, E_g and T_{2g} , give three A' and two A'' states in C_s symmetry. Since the band polarization ratios imply that at least two of the spin-allowed bands are due to transitions between states which belong to the same irreducible representation, the ground state must be an A' state; this fixes the upper states of the labelled $M(4)$ Fe^{2+} transitions. One would then expect two spin-allowed $A' \rightarrow A''$ transitions; the 4200 cm^{-1} band is due to one and, since the 8000 cm^{-1} band is strongly α -polarized, it is probably due to the other such transition.

The bands between 18770 and 21030 cm^{-1} , except for that at $20210\text{--}20250\text{ cm}^{-1}$, form an approximate arithmetical progression with an interval of $400 \pm 50\text{ cm}^{-1}$. This suggests that the weaker bands in the progression are related to the $M(4)$ Fe^{2+} band at $19950\text{--}19970\text{ cm}^{-1}$. Perhaps they are due to the same transition occurring at non- $M(4)$ sites.

The polarization of the $26200\text{--}26300\text{ cm}^{-1}$ band

implies that it cannot be due to an $M(4)$ transition; it may also be due to an Fe^{2+} transition at another site. The narrow band at 26950 cm^{-1} may be due to Fe^{3+} . It has a position and width characteristic of the ${}^6A_{1g} \rightarrow {}^4E_g$ transition, its polarization ratio is consistent with that of a transition at $M(4)$, the preferred Fe^{3+} site in rhodonite, and its oscillator strength need not be higher than that observed in pyralspite garnets (Moore and White, 1972). The strong absorption above 30000 cm^{-1} is also due mainly to iron, probably to a charge-transfer band.

The Fe^{2+} bands above 16000 cm^{-1} are generally weak, and it is possible that many are "swamped" by neighboring Mn^{2+} bands.

Manganese Bands. The bands not produced by Fe^{2+} , Fe^{3+} , or charge transfer are probably due to Mn^{2+} . The bands near 24000 cm^{-1} and 29000 cm^{-1} are relatively sharp and occur near the expected energies for the field-independent transitions, so that they are probably due to the transitions corresponding to ${}^6A_{1g} \rightarrow {}^4E_g$ and ${}^6A_{1g} \rightarrow {}^4E_g$ in O_h symmetry. The other intense bands are probably due to transitions arising from transitions to ${}^4T_{1g}$ and ${}^4T_{2g}$ in O_h . For the 24700 and 25200 cm^{-1} bands these criteria do not give an unambiguous assignment.

The weak bands between 24900 and 25800 cm^{-1} are probably also due to Mn^{2+} , as a group of bands of similar width and relative intensity was observed by Keester and White (1968) in low-iron rhodochrosite on the high-frequency side of the band arising from the ${}^6A_{1g} \rightarrow {}^4E_g$ transitions. Unlike the rhodonite bands, those in rhodochrosite were resolved at room temperature, but this is not an important difference. It arises because the background absorbance below these bands is greater in high-iron rhodonite than in low-iron rhodochrosite and so swamps these bands in high-iron rhodonite at room temperature. The absence of some of these bands from the Danglemar low-iron rhodonite spectra is due to the small size of the crystals causing the bands to be lost in the noise.

The important difference between the manganese spectra of the two rhodonites shown by Figure 5 is the occurrence of bands at 24510 and $27950\text{--}28020\text{ cm}^{-1}$, and perhaps at $21200\text{--}21500\text{ cm}^{-1}$, in the Danglemar low-iron rhodonite spectrum which do not correspond to any high-iron rhodonite bands. The simplest explanation is that these bands are due to transitions at the preferred Ca^{2+} site, $M(5)$; because of the difference between the calcium con-

tent of the two rhodonites, the proportion of $M(5)$ sites occupied by Mn^{2+} will be much higher in the Danglemar low-iron rhodonite. The oscillator strengths tend to be larger in the Danglemar low-iron rhodonite crystal, suggesting that exchange interactions among neighboring Mn^{2+} ions contribute to the intensity of some bands.

Another difference between the spectra is that in high-iron rhodonite the 24300 and 24450 cm^{-1} band intensities in certain polarizations increase by 20 to 40 percent between 12 K and 50 K with little change above 50 K, whereas the corresponding Danglemar low-iron rhodonite bands are temperature-independent. No explanation can be suggested at this stage.

The splittings of O_h transitions are too large to be due to spin-orbit interaction (see Goode, 1963). Coupling between a ground state vibration and an electronic transition is an unlikely explanation of the splittings. Except for the high-iron rhodonite bands mentioned above, band intensities do not change within experimental error between 18 K and room temperature, while the almost constant intensity of the temperature-dependent bands above 50 K would not be expected for a band arising from coupled transitions. The splittings can be explained by the low crystal-field symmetry and the multiplicity of sites, but not by one of these alone. Manganese compounds with one type of site, such as spessartite, may exhibit two bands corresponding to ${}^6A_{1g} \rightarrow {}^4E_g$ (Moore and White, 1972) so that the splitting of at least this O_h transition cannot be due to a multiplicity of sites alone. Conversely, splitting by the low field symmetry cannot explain why the low-iron rhodonite spectra exhibit five bands corresponding to the higher ${}^6A_{1g} \rightarrow {}^4T_{2g}$ transition.

Conclusion

Band wavenumbers at room temperature and 18 K, and the polarization ratios and absolute intensities at 18 K of high-iron rhodonite bands above 3000 cm^{-1} have been listed in Table 2. Cooling increases the number of distinguishable bands.

The principal axis directions for the high-iron rhodonite refractive index indicatrix are fixed in the crystal within 10–20° between 2000 and 31000 cm^{-1} and agree with those of Overton (1968). For a low-iron rhodonite (100) cleavage slice there is a shift of $10 \pm 3^\circ$ in the axis directions near 20000

cm^{-1} and the axis directions differ by 20–30° from those predicted by Overton's measurements.

Comparisons among the vibrational spectra of rhodonites of different compositions suggest that the bands between 330 and 470 cm^{-1} come from vibrations heavily involving ions at some or all of $M(1)$ – $M(4)$ or $M(1)$ – $M(5)$ and those between 490 and 1100 cm^{-1} from vibrations heavily involving silicate groups. Comparing low-iron and high-iron rhodonite spectra permits most non-vibrational bands to be assigned to Fe^{2+} or Mn^{2+} (Table 2). Mn^{2+} dominates the electronic spectrum between 16000 and 30000 cm^{-1} , iron outside these limits. Generally, several Mn^{2+} bands correspond to one O_h transition, the splitting being probably due to a combination of site multiplicity and the low field symmetry. Polarized spectra showed which bands could be due to charge transfer and permitted tentative classification of the stronger $Fe^{2+} d \rightarrow d$ bands to be carried out on the basis of approximate C_s symmetry of the $M(4)$ site.

Acknowledgments

We wish to thank Dr. I. M. Threadgold of the University of Sydney for supplying the high-iron rhodonite; the Geology Department, Australian National University, for supplying the Cornwall rhodonite; and the Research School of Earth Sciences, Australian National University, for the electron microprobe analyses.

References

- AGIORGITIS, G. (1969) Investigations of manganese minerals by differential thermoanalysis and infrared spectroscopy. *Tschermaks Mineral. Petrogr. Mitt. Ser. 3*, **13**, 273–283.
- ALLEN, G. C., AND N. S. HUSH (1967) Intervalence-transfer absorption. Part 1. Qualitative evidence for intervalence-transfer absorption in inorganic systems in solution and in the solid state. *Progr. Inorg. Chem.* **8**, 357–389.
- BLOSS, F. D. (1971) *Crystallography and Crystal Chemistry—An Introduction*. Holt, Rinehart and Winston, Inc., New York.
- DEER, W. A., R. A. HOWIE, AND J. ZUSSMAN (1963) *Rock-forming Minerals*. Vol. II, *Chain Silicates*. Longman Group, Ltd., London.
- GOODE, D. H. (1963) Optical absorption spectrum of Mn^{2+} in cubic and tetragonal ligand fields. *J. Chem. Phys.* **43**, 2830–2839.
- GOSSNER, B., AND K. BRÜCKL (1928) Structural relations of rhodonite to other silicates. *Centralbl. Mineral. Geol. Paläontol. Abt. A*, 316–322.
- HUSH, N. S. (1967) Intervalence-transfer absorption. Part 2. Theoretical considerations and spectroscopic data. *Progr. Inorg. Chem.* **8**, 391–444.
- KEESTER, K. L., AND W. B. WHITE (1968) Crystal-field spectra and chemical bonding in manganese minerals. In P. Gay, A. F. Seager, H. F. W. Taylor, and J. Zussman,

- Eds., *Int. Mineral. Assoc., Pap. Proc. Fifth General Meet., Cambridge, 1966*. The Mineralogical Society, London, p. 22-35.
- LAKSHMAN, S. V. J., AND B. J. REDDY (1973) Optical absorption spectrum of Mn^{2+} in rhodonite. *Physica*, **66**, 601-610.
- LAZAREV, A. N., AND T. F. TENISHEVA (1961) Vibrational spectra of silicates. III. Infrared spectra of the pyroxenoids and other chain metasilicates. *Opt. Spektrosk.* **11**, 584-587. [transl. *Opt. Spectrosc.* **11**, 316-317 (1961)].
- MANNING, P. G. (1968) Absorption spectra of the manganese-bearing chain silicates pyroxmangite, rhodonite, bustamite, and serandite. *Can. Mineral.* **9**, 348-357.
- MOORE, R. K., AND W. B. WHITE (1972) Electronic spectra of transition metal ions in silicate garnets. *Can. Mineral.* **11**, 791-811.
- OVERTON, R. (1968) *A Study of Some Single Crystals of Rhodonite from Broken Hill, New South Wales*. B.Sc. (Hons.) Thesis, University of Sydney, N.S.W.
- PEACOR, D. R., AND N. NIIZEKI (1963) The redetermination and refinement of the crystal structure of rhodonite, $(Mn,Ca)SiO_3$. *Z. Kristallogr.* **119**, 98-116.
- RAMACHANDRAN, G. N., AND S. RAMASESHAN (1961) Crystal optics. In, S. Flügge, Ed., *Handbuch der Physik*, Vol. XXV/1. Springer-Verlag, Berlin, p. 1-217.
- RUTSTEIN, M. S., AND W. B. WHITE (1971) Vibrational spectra of high-calcium pyroxenes and pyroxenoids. *Am. Mineral.* **56**, 877-887.
- WARD, J. C. (1955) Measurements of ultra-violet dichroism. *Proc. Royal Soc. A* **228**, 205-219.
- WILKINS, R. W. T., AND W. SABINE (1973) Water content of some nominally anhydrous silicates. *Am. Mineral.* **58**, 508-516.
- WILSON, E. B., J. C. DECIUS, AND P. C. CROSS (1955) *Molecular Vibrations*. McGraw-Hill, New York.

Manuscript received, October 12, 1973; accepted for publication, August 2, 1974.